Acta Materialia 232 (2022) 117943

Contents lists available at ScienceDirect

Acta Materialia

journal homepage: www.elsevier.com/locate/actamat

Asymmetric $(11\bar{2}1)[11\bar{2}\bar{6}]$ twin boundary and migration mechanism in hexagonal close-packed titanium

Bin Li*, Kefan Chen

Department of Chemical and Materials Engineering, University of Nevada, Reno, NV 89557, USA

ARTICLE INFO

Article history:
Received 8 December 2021
Revised 20 February 2022
Accepted 13 April 2022
Available online 15 April 2022

Key words:
Twinning
Shuffling
Twinning dislocation

ABSTRACT

Classical twinning theory predicted that a simple shear was able to create a perfect, twinned structure without the need of atomic shuffles for $(11\bar{2}1)[11\bar{2}\bar{6}]$ twinning mode in hexagonal close-packed (HCP) metals, and the elementary twinning dislocation should be a two-layer zonal. However, it was revealed in the literature that this particular twinning mode could not have mirror symmetry between the parent and twin, and shuffles should be involved during twin boundary (TB) migration. These conflicting reports indicate that the $(11\bar{2}1)[11\bar{2}\bar{6}]$ twinning mechanism has not been completely resolved, and what configuration of twinning dislocation mediates twin growth is not well understood either. In this work, atomistic simulation is conducted to further understand the twinning mechanism in titanium. Novel structural analyses are performed to reveal how the parent lattice is transformed to the twin lattice. The results show that the mirror symmetry of a perfect, unrelaxed TB breaks down after relaxation, because of the very high repulsive force between the atom pairs on mirrored positions with a spacing less than half of the lattice constant. As a result, the stacking sequence of the twin differs from that of the parent after relaxation. During twin growth, each $\{1\bar{1}00\}$ prismatic plane of the parent splits into two layers and reorganize into the prismatic planes of the twin, such that the twin prismatic are no longer aligned with the parent prismatic and the mirror symmetry breaks down. This process is accomplished by atoms shuffling in the opposite direction that is perpendicular to the twinning shear. The atomic shuffles spread over multiple consecutive twinning planes to minimize the shuffling magnitude on each twinning plane. Thus, the actual TB is no longer a single twinning plane, but a multi-layer interface zone. Careful examination shows that no well-defined twinning dislocation core can be identified, although single-layer steps can still be observed.

1. Introduction

Twinning plays a vital role in mechanical properties of metals with hexagonal close-packed (HCP) crystal structures. All the twinning planes in HCP metals are not close-packed, i.e. they are either the first order or the second order pyramidal planes. Therefore, twinning is a very important deformation mode that is able to accommodate plastic strain along the *c*-axis of HCP materials [1–8]. There are four major twinning modes in HCP metals: $(10\bar{1}2)[10\bar{1}\bar{1}]$, $(10\bar{1}1)[10\bar{1}\bar{2}]$, $(11\bar{2}2)[11\bar{2}\bar{3}]$, $(11\bar{2}1)[11\bar{2}\bar{6}]$, with the $(10\bar{1}2)[10\bar{1}\bar{1}]$ mode being the most commonly observed in all HCP metals. The individual twinning modes vastly differ from one mode to another in terms of atomic shuffles, core structure and configuration of twinning dislocations [9–13]. In contrast to twinning in metals with cubic crystal structures in which twin nucleation and growth are mediated by well-defined partial dislocation on twin boundaries (TBs) [14–16], twin growth in HCP metals is often mediated by zonal twinning dislocations that simultaneously involve multiple twinning planes [2,5,8,17–19]. Additionally, a homogeneous shear alone is unable to complete the twinning process and atomic shuffling is required to achieve the correct twin orientation relationship [1,2,20,21]. In predicting possible twinning modes in classical twinning theory [1,2], a general, qualitative rule is that a small magnitude of twinning shear *s* and simple atomic shuffles are preferred. However, this rule, seemingly simple enough, has turned out to be quite complicated. Questions arise such as how small is small and how simple is simple for a specific twinning mode. For a typical example of $(11\bar{2}2)[11\bar{2}\bar{3}]$ mode in Ti, it has been widely accepted that the second invariant plane or K_2 plane is $\{11\bar{2}4\}$ which corresponds to a small *s* of ~0.22 and very complex shuffles, but the most recent scanning transmission electron microscopy (STEM) work [22] and all the atomistic simulations in the literature [5,22,23] show that the actual K_2 plane is (0002) which corresponds to a much larger *s* (~0.66) but a much simpler shuffle along the direction of twinning shear. Thus, careful analy-

* Corresponding author
E-mail address: binl@unr.edu (B. Li).

https://doi.org/10.1016/j.actamat.2022.117943
1359-6454/

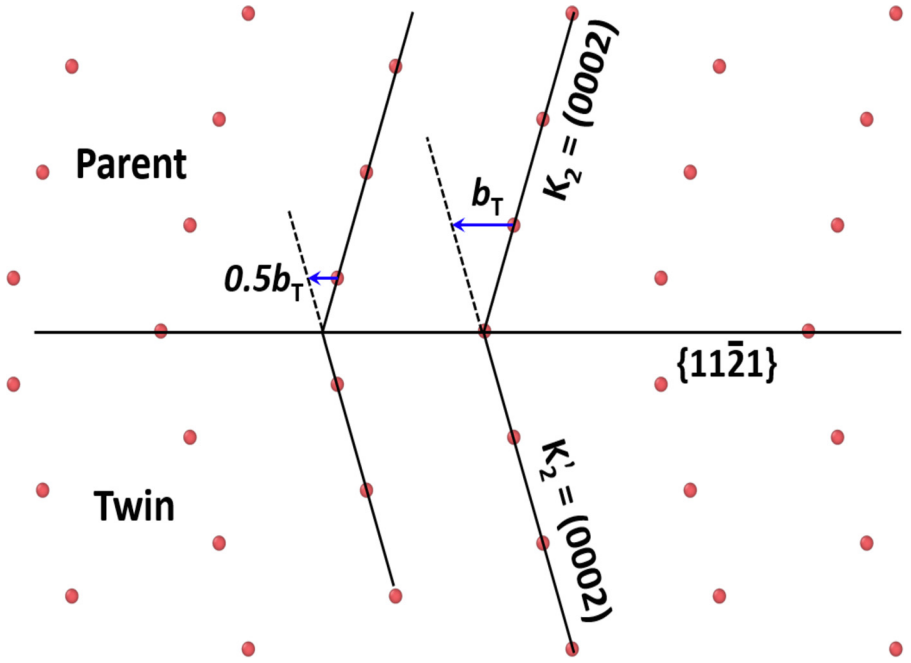

Fig. 1. The twinning elements for $\{11\bar{2}1\}11\bar{2}\bar{6}$ mode as predicted in the classical twinning theory. The elementary twinning dislocation b_T is predicted to be a two-layer zonal dislocation, which comprises two twinning planes simultaneously. A simple shear mediated by b_T moves two layers of atoms to the twin sites.

ses are required to resolved the twinning mechanism for individual modes [24].

For titanium (Ti) and zirconium (Zr) and other HCP metals, twinning mode $(11\bar{2}1)[11\bar{2}\bar{6}]$ has been observed and reported in experiments [25–29]. Fig. 1 shows the twinning elements predicted in the classical theory [1,2]. The twin and the parent are in perfect mirror symmetry and the twin structure is not relaxed. This twinning mode has a twinning shear with a magnitude of $s = 1/\gamma$ (γ is the c/a ratio, 1.588 for Ti). For Ti, $s = 0.63$. The magnitude of the Burgers vector (b_T) of the elementary twinning dislocation equals $a/\sqrt{1+4\gamma^2} \approx 0.89$ Å (a is the lattice constant of Ti, 2.95 Å), which should be a two-layer zonal dislocation. On each twinning plane, the magnitude is ~0.45 Å or $0.5b_T$. No atomic shuffles are required because a homogeneous shear is able to carry all parent atoms to the twin lattice [2], as it can readily be seen in Fig. 1. When a simple shear is applied parallel to the twinning plane, the twin boundary (TB) migrates upward into the parent by two $\{11\bar{2}1\}$ planes via a two-layer zonal dislocation, and the parent atoms exactly reach the sites of the twin lattice. However, this is not the case for a relaxed TB.

The interfacial structure of a $(11\bar{2}1)[11\bar{2}\bar{6}]$ TB was studied in a number of atomistic simulations [6,10,30,31]. Using a truncated Lennard-Jones potential in their simulations, Minonishi et al. [6] showed that the mirror symmetry of twins broke down because alternate basal planes of the twin were displaced normal to the plane of shear and no zonal twinning dislocations were necessary. They also suggested that atomic shuffles were needed due to the change in stacking sequence in the twin. In this pioneer work, no simulations were performed to investigate how the TB migrated under loading. Thus, how the parent lattice is dynamically transformed to the twin lattice and exactly what atomic shuffles and what twinning dislocations are involved still remain unclear. Serra and Bacon [30] simulated the structure of the $\{11\bar{2}1\}$ twinning dislocations and found that it had a very wide core, spreading over the relaxable interface region, and the width of the core disregistry was as large as ~75b. They also claimed that no atomic shuffles were required to move atoms to the correct sites in the twin, and a simple shear by the twinning dislocation could generated the correct twin structure.

The discrepancies in the literature in terms of TB structure, configuration of twinning dislocations and atomic shuffles warrant further investigations, so that the twinning mechanism of $(11\bar{2}1)[11\bar{2}\bar{6}]$ mode can be better understood. The purpose of this work is to study the TB structure and migration, as well as the configuration of TB defects of $(11\bar{2}1)[11\bar{2}\bar{6}]$ twinning mode, using novel structural analyses in molecular dynamics simulations. The results obtained provide new insight on the twinning mechanisms in HCP metals.

2. Simulation method

The interatomic potentials for Ti used in this work were developed by Mishin *et al.* [32]. The embedded atom method (EAM) type potential [33,34] was created for Ti-Al alloys. Using the potentials for Ti, we simulated $(11\bar{2}2)[11\bar{2}\bar{3}]$ twinning in Ti [5,22,35], pyramidal dislocation slip and $(11\bar{2}1)[11\bar{2}\bar{6}]$ twinning, and the results were satisfactory. In this work, we use the same potentials to simulate the TB structure and TB migration of $(11\bar{2}1)[11\bar{2}\bar{6}]$ mode. Large-scale Atomic/Molecular Massively Parallel Simulator or LAMMPS [36] is used for our simulation. Visualization tool OVITO [37] is used to analyze the structural evolution during twinning.

Fig. 2 shows the initial configuration of the twins after relaxation in our atomistic simulations. The twins are constructed such that the two crystals satisfy the perfect $(11\bar{2}1)[11\bar{2}\bar{6}]$ twin orientation relationship. The box size is 35 nm × 30 nm × 30 nm, containing a total of ~1.8 million atoms. Free surfaces are applied to all three dimensions. After relaxation, a shear strain is applied by moving the two layers of atoms on the top surface at a constant velocity of 0.1 Å/ps, which corresponds to a strain rate of 2.86×10^8 /sec, while the two layers of atoms on the bottom surface are fixed. The temperature in the simulation is maintained at 5 K to reduce thermal noise in structural analyses, by applying the Nosé–Hoover [38,39] thermostat to the system

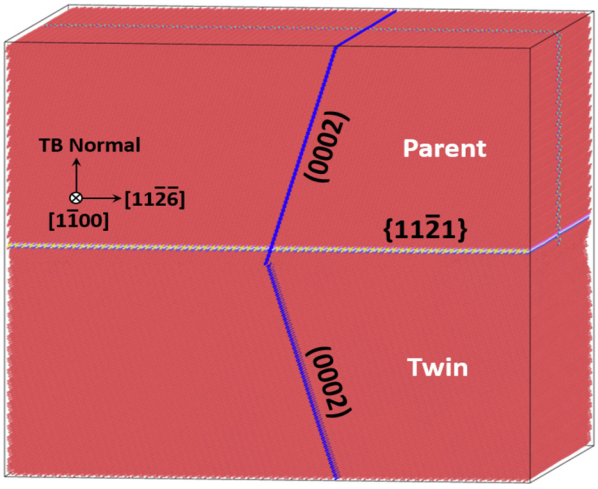

Fig. 2. The initial system of (11$\bar{2}$1)[11$\bar{2}\bar{6}$] twins. To track structural evolution during twin boundary migration, multiple {11$\bar{2}$1} twinning planes, the (0001) basal and {1$\bar{1}$00} prismatic planes are colored differently before a shear strain is applied. The color pattern is retained throughout the simulation so that structural change can be tracked unambiguously.

during shear deformation. Although the strain rate in atomistic simulations is typically many orders of magnitude faster than in experiments, for dislocation structures and energies that are rate independent, the strain rate is still able to generate results of physical significance.

As shown in Fig. 2, a special color scheme is used in our simulation. Five consecutive {11$\bar{2}$1} twinning planes on the parent side are pre-selected and colored differently. A (0002) basal plane of parent and a basal plane of twin are also pre-selected and colored in blue. Additionally, three consecutive {1$\bar{1}$00} prismatic planes on the parent side are pre-selected and colored in green, red and blue (a magnified side view of these pre-selected prismatic planes is provided below). This color scheme is retained throughout the simulation such that the lattice transformation, TB migration and structural evolution during twinning can readily be recognized and tracked without ambiguity. This strategy is crucial for structural analyses.

3. Simulation results

3.1. The structure of the relaxed {11$\bar{2}$1} twin boundary

First, we closely analyze the structure of the unrelaxed and the relaxed {11$\bar{2}$1} TB. The radial distribution function (RDF) of the unrelaxed TB with perfect mirror symmetry is shown in Fig. 3a. RDF represents the probability of finding a pair of atoms within a specific spacing. Careful examination shows that a very small peak appears at the spacing of 1.4 Å (see the inset). These atom pairs are located on both sides of the TB and are on the mirrored positions (connected by the short blue bonds). This spacing is less than half of the equilibrium lattice parameter of Ti (2.95 Å), and results in a very strong repulsive force between the two atoms of a pair. Calculation of the energy of the unrelaxed TB shows a value of 11.88 J/m^2, which is exceptionally high for a symmetric high angle grain boundary. Consequently, the perfect TB with a mirror symmetry is unstable.

After relaxation, the very small peak at 1.4 Å disappears, as shown in Fig. 3b. The atoms at this small spacing are pushed away by the repulsive forces and the structure of the TB is reorganized into a new one. The TB energy drastically decreases to 171 mJ/m^2. The interatomic spacing of those atoms near the relaxed TB now falls in the range of 2.7~2.82 Å (the blue bonds) which is only slightly shorter than the equilibrium lattice parameter (see the inset). When viewed along the zone axis [1$\bar{1}$00] of the twins, the TB structures seems to be similar to that of the unrelaxed TB (Fig. 3a), but the TB structure actually no longer has a mirror symmetry, as seen below.

Fig. 4a shows the structure of the unrelaxed TB when viewed along the direction of twinning shear, i.e., side view of the twins along the [11$\bar{2}\bar{6}$]. The double-layered (1$\bar{1}$00) prismatic planes of the parent and twin are perfectly aligned along the TB normal direction. The parent and the twin lattice are perfectly mirrored by the TB plane. In stark contrast, after relaxation, the mirror symmetry breaks down, as shown in Fig. 4b. The original sharp interface now becomes diffuse and the TB is no longer a plane, but an interface zone that spreads over multiple (11$\bar{2}$1) planes. A salient feature in Fig. 4b is that the columns of (1$\bar{1}$00) prismatic planes of the parent and those of the twin are no longer aligned but become misaligned. The misalignment is denoted by the solid and the dashed green lines which marks the traces of the double layers of individual prismatic planes in the parent and twin. It appears that the individual prismatic planes of the parent, which have two layers of atoms, split and then reorganize into the prismatic planes of the twin. This new TB structure is produced as a result of the very high repulsive force between those short-bonded atoms near a perfect TB with mirror symmetry (Fig. 3a).

3.2. Twin boundary migration

Under the applied shear strain, the TB migrates upward (indicated by the block arrow), as shown in the 2D view of the TB in Fig. 5. Only a thin slice (6 Å thick) is shown along the [1$\bar{1}$00] zone axis direction. The TB is displayed as light-gray atoms in the common neighbor analysis (CNA) [40]. It can be seen that during TB migration, the pre-selected basal plane of the parent, which is colored in blue, is deflected and becomes the basal plane of the twin. Therefore, the lattice transformation can be described as: $(0002)_P \rightarrow (0002)_T$. Thus, the second invariant plane is indeed (0002), which is exactly the same as the prediction of the classical twinning theory. It appears that, in the $(0002)_P \rightarrow (0002)_T$ lattice transformation, the parent atoms are directly sheared to the twin positions, and no atomic shuffles are involved. However, the stacking sequence in the parent and in the twin has changed after the TB traverses through.

To show the change in stacking sequence after twinning, two neighboring (0002) basal plane in the parent are selected and colored in green and red, as shown in Fig. 6. Only a small region that contains the TB is displayed. To reveal the stacking sequence of the parent, first, the basal planes are tilted such that the viewing direction is along the [0001], i.e. the *c*-axis of the parent lattice (Fig. 6a). The TB is now inclined with viewing direction. A hexagonal motif is delineated by the green lines. The red (0002) plane is projected onto the green (0002) plane. A triangle that connects the red atoms inside the hexagonal motif is delineated. Next, the two basal planes are tilted such that the viewing direction is along the [0001] of the twin lattice (Fig. 6b). Similarly, the basal hexagonal motif of the green plane is delineated by the green lines. However, the projected positions of the red atoms on the green (0002) plane have changed, as denoted by the red triangle inside the hexagonal motif. If we denote the stacking sequence in the parent as …*ABABAB*…, then the stacking sequence in the twin has changed to …*ACACAC*… after twinning.

Fig. 6a and b also reveal the misalignment of individual prismatic columns in the parent and in the twin. To better understand what happens to the prismatic planes during TB migration, we focus on the three pre-selected prismatic planes in the parent and track the changes to these prismatic planes. Fig. 7 shows the three pre-selected prismatic planes that colored in green, red and blue

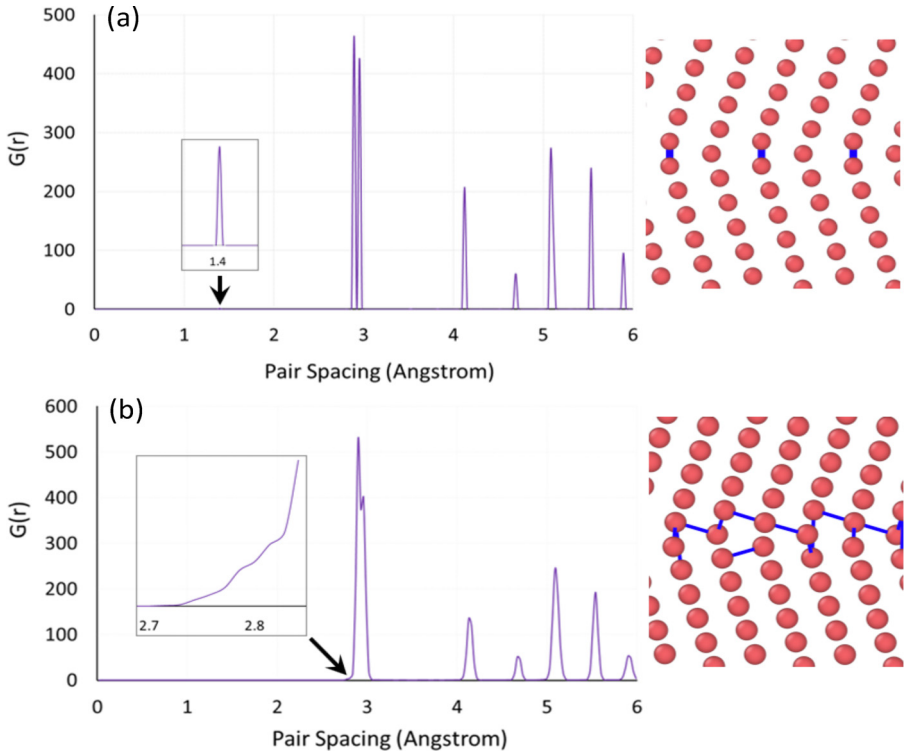

Fig. 3. (a) Radial distribution function (RDF) of a perfect $(11\bar{2}1)[11\bar{2}\bar{6}]$ twin boundary with mirror symmetry. Short atom pairs appear at 1.4 Å which is less than half of the lattice constant 2.95 Å (the inset). These bonds are shown in blue in the atomic structure. (b) After relaxation, the short bonds disappear and are rearranged into bonds with spacings between 2.7~2.82 Å at the twin boundary (indicated by the blue bonds in the inset).

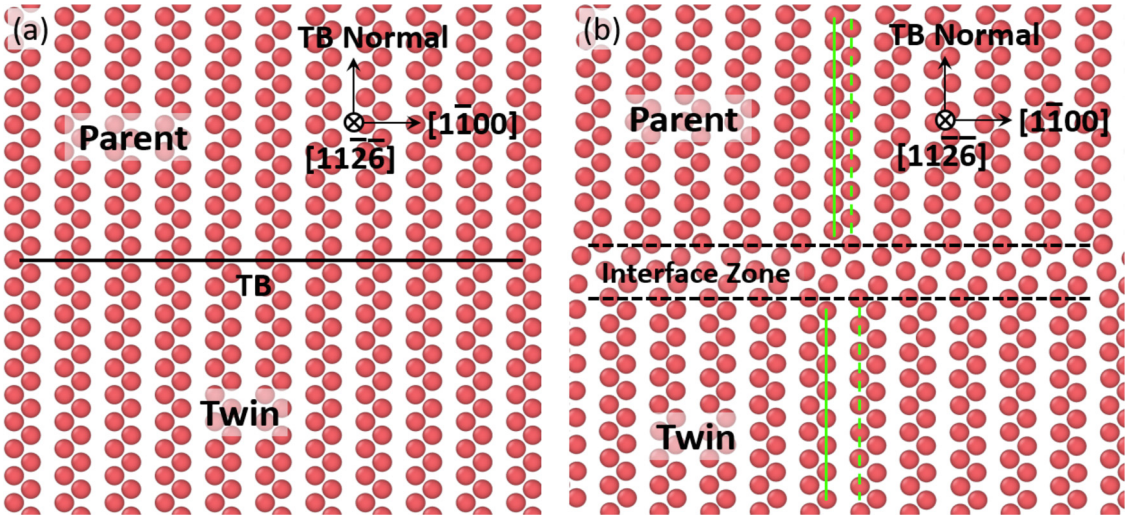

Fig. 4. (a) Twin structure with a perfect twin boundary before relaxation when viewed along the direction of twinning shear $[11\bar{2}\bar{6}]$. The double-layered columns are $(1\bar{1}00)$ prismatic planes. A perfect mirror symmetry can be seen about the twin boundary. (b) After relaxation, the mirror symmetry breaks down. The twin boundary plane becomes a zone with a distorted structure. Note that the prismatic columns in the twin are shifted and no longer aligned with the prismatic columns in the parent.

and how they evolve during TB migration in time sequence. The viewing direction is along the $[11\bar{2}\bar{6}]$, i.e. the direction of twinning shear. Fig. 7a shows the initial structure of the prismatic planes, each of which contains double layers of atoms because each prismatic plane is actually comprised of atoms that reside on two slightly separated planes with a spacing of $\frac{\sqrt{3}}{6}a$. At 40 ps, the TB is migrating into these pre-selected prismatic planes as the parent lattice is transformed into the twin lattice. It can clearly be seen that each double-layered prismatic plane is splitting and reorganizing into the prismatic planes of the twin. For example, the two layers of green atoms separate and move in the opposite direction, and so do the two layers of red atoms on the neighboring prismatic plane. Eventually, the green atoms moving toward the right and the red atoms moving toward the left combine and reorganize into a new prismatic plane that contains mixed colors. This process is accomplished by atomic shuffling and occurs to all the prismatic planes of the parent, giving rise to the misaligned structure that is shown in Fig. 4 and 6.

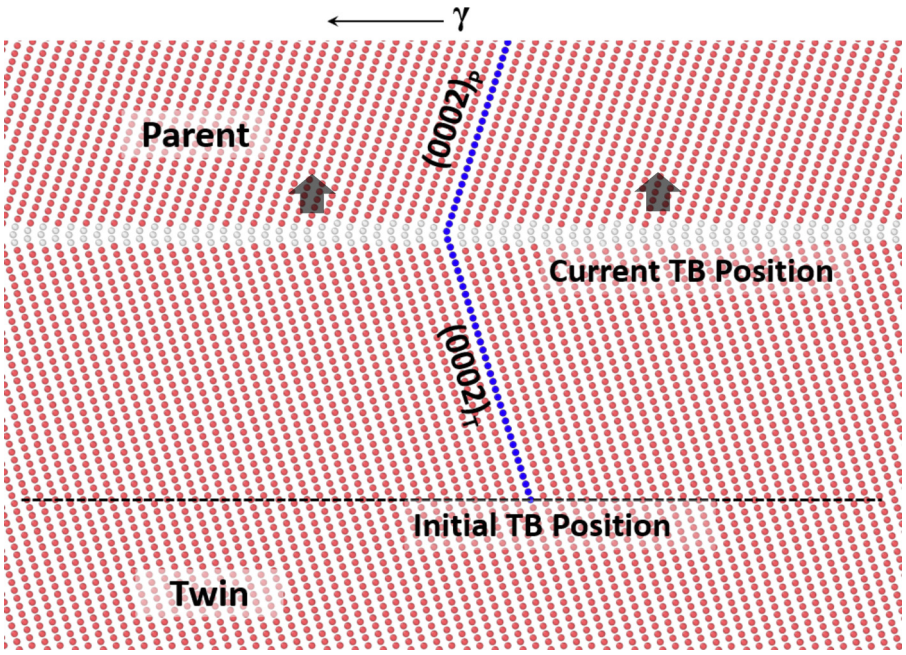

Fig. 5. Under the applied shear strain, the twin boundary migrates upward. The atoms on the twin boundary are colored in gray. As indicated by the blue atoms, the atoms of the parent basal are being aligned to the twin basal, indicating that the second invariant plane K_2 is (0002).

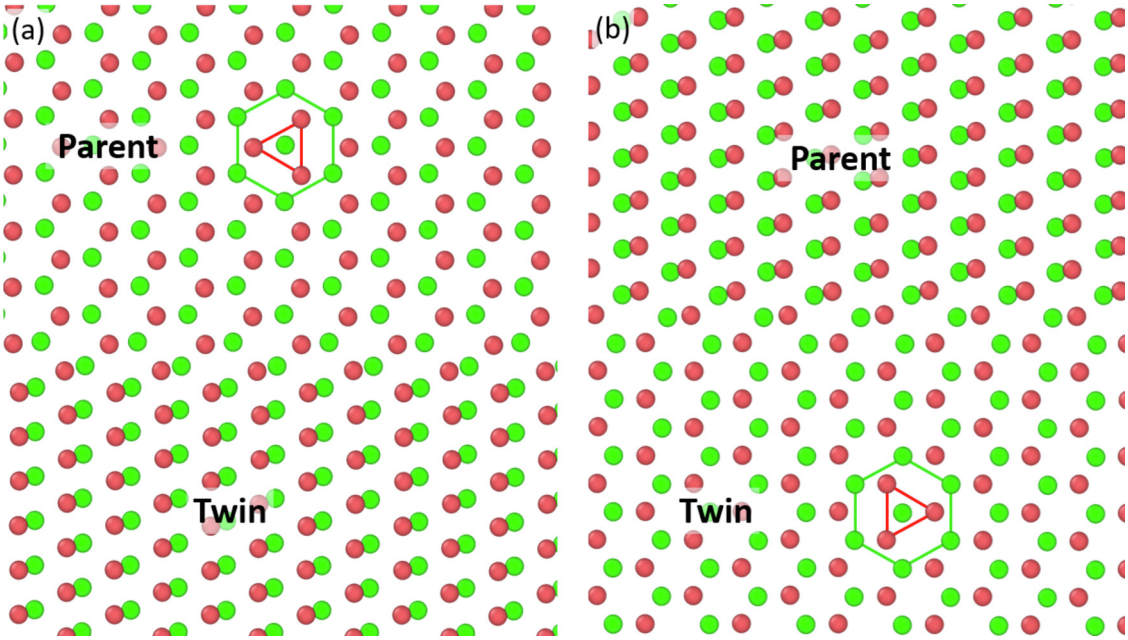

Fig. 6. (a) The stacking sequence in the parent crystal. Only two basal planes are shown and the viewing direction is along the [0001] of the parent lattice. The twin boundary plane is now inclined with the viewing direction. (b) The stacking sequence in the twin crystal. The viewing direction is now tilted to the [0001] of the twin lattice. Note that the stacking sequence in the twin has changed.

To further reveal the split of the parent prismatic planes and the following reorganization into new prismatic planes of the twin, we take three consecutive, pre-selected twinning planes and examine the structure evolution of these planes after the TB traverses through. The plot is shown in Fig. 8a and b. In these plots, the viewing direction is along the twinning plane normal. From top down, the three consecutive $\{11\bar{2}1\}$ planes are colored in pink, yellow and light-gray. The structural motifs of the $\{11\bar{2}1\}$ planes are denoted by the colored hexagons. The traces of the $(1\bar{1}00)$ prismatic planes are denoted the by the pairs of dashed and dotted green lines which represent their double-layered structure (Fig. 8a). The dotted lines run across the yellow atoms, whereas the dashed lines run across the pink and the light-gray atoms. During twinning, the dotted and the dashed lines of a prismatic plane move in opposite direction, as indicated by the black arrows. Then the dashed lines join the dotted lines from the neighboring prismatic plane, such that the split layers are reorganized into the prismatic planes of the twin (Fig. 8b). It can also be seen in Fig. 8b that, after twinning, the pink hexagon, which resides originally to the left of the light-gray hexagon before twinning (Fig. 8a), has moved to the right. The displacement corresponds to the magnitude of the theoretical

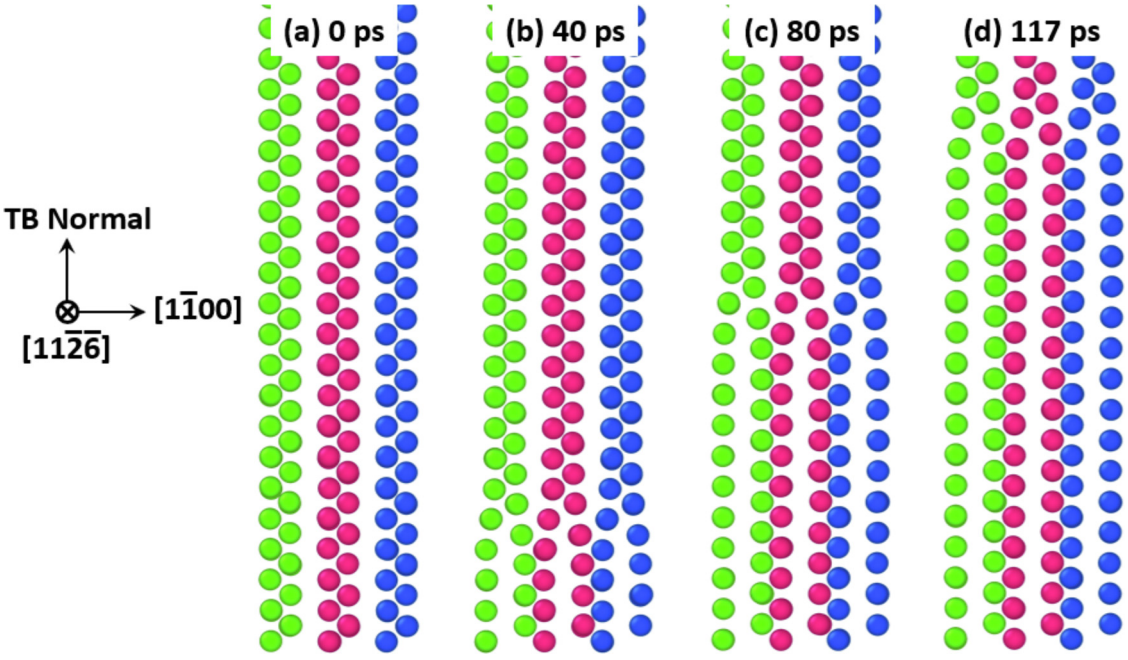

Fig. 7. Evolution of three prismatic columns colored in green, red and blue. The viewing direction is along the [11$\bar{2}\bar{6}$], i.e., the direction of twinning shear. During twin boundary migration, each of the (1$\bar{1}$00) prismatic planes of the parent, which has a double-layered structure, splits into two layers that move in the opposite direction, and then reorganize into the prismatic planes of the twin that are now misaligned with the prismatic planes in the parent. (For interpretation of the references to colour in this figure legend, the reader is referred to the web version of this article.)

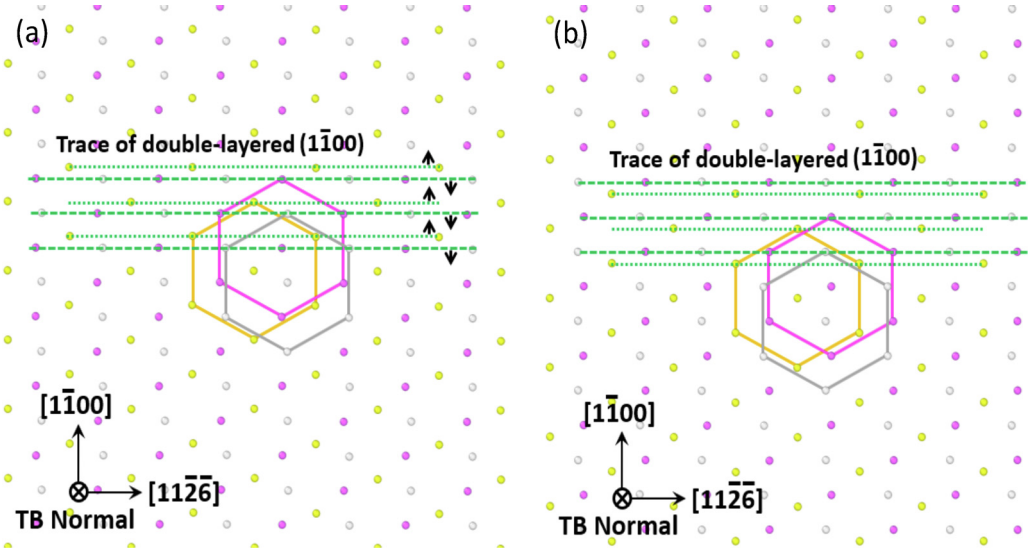

Fig. 8. Shear and shuffle in (11$\bar{2}$1)[11$\bar{2}\bar{6}$] twinning. The viewing direction is along the twinning plane normal. Three successive {11$\bar{2}$1} planes are pre-selected and colored in pink, yellow and light-gray. (a) Before twinning. The black arrows indicate the split of the double-layered (1$\bar{1}$00) prismatic planes which are denoted by the dotted and the dashed green lines. (b) After twinning. Note the change in relative position of the colored twinning planes, and the split and reorganization of the prismatic planes. (For interpretation of the references to colour in this figure legend, the reader is referred to the web version of this article.)

elementary twinning Burgers vector, i.e. $a/\sqrt{1+4\gamma^2}$, for every two twinning planes.

4. Analysis and discussion

4.1. Defects on the moving twin boundary

Twinning dislocations in HCP metals are typically zonal twinning dislocations, according to the classical twinning theory. The height of a zonal twinning dislocation is defined as the number of twinning planes that are comprised between the TB and the twinning plane that intersects the K_2 plane at a lattice point. This concept was proposed by Thompson and Millard [19] to describe the twinning dislocation in (10$\bar{1}$2)[10$\bar{1}\bar{1}$] mode. They showed that the twinning dislocation for this twinning mode in Cd should comprise two {10$\bar{1}$2} planes simultaneously. However, this prediction is at odds with most experimental observations and atomistic simulations in which the actual TB hugely deviates from the {10$\bar{1}$2} twinning plane [12,20,21,41–43]. The classical theory is unable to account for such an abnormal behavior. Bilby and Crocker [1], Christian and Mahajan [2] showed that the twinning dislocation for (11$\bar{2}$2)[11$\bar{2}\bar{3}$] mode should be a three-layer zonal twinning dislocation, which corresponds to the K_2 plane of {11$\bar{2}\bar{4}$}. But this prediction has been proven incorrect by recent experiments which

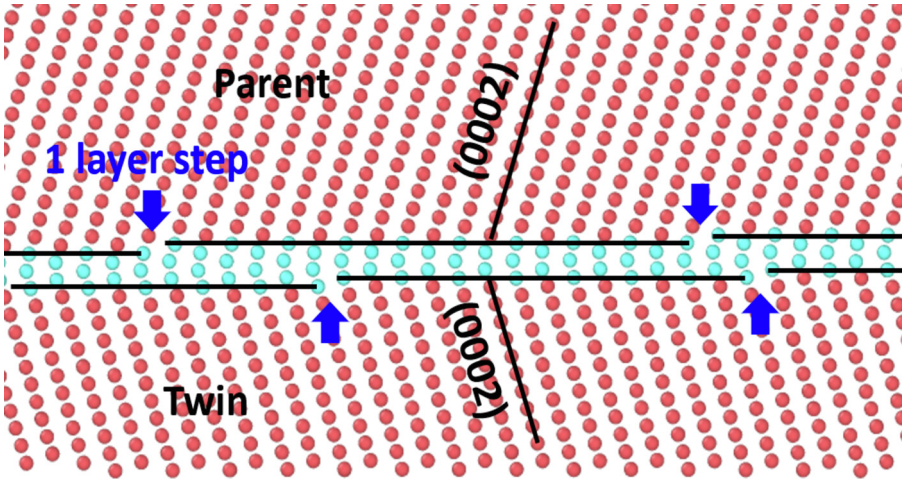

Fig. 9. A magnified view of the moving twin boundary (TB) in common neighbor analysis (CNA). The TB is actually a zone of atoms (colored in cyan) that do not have HCP structure. One-layer steps (indicated by the blue block arrows) can still be recognized in this 2D view; however, they do not have the characteristics of twinning dislocations (see Fig. 10). (For interpretation of the references to colour in this figure legend, the reader is referred to the web version of this article.)

show that the twinning dislocation only contains a single layer [22]. The classical theory predicted that the twinning dislocation of $(10\bar{1}1)[10\bar{1}\bar{2}]$ mode should be a two-layer or a four-layer zonal twinning dislocation, and this prediction was confirmed in atomistic simulation by Li and Ma [8]. They showed that, indeed, a four-layer zonal twinning dislocation mediating $(10\bar{1}1)[10\bar{1}\bar{2}]$ twin growth in magnesium dissociated into two two-layer partial zonal twinning dislocations.

In the prediction of the classical theory, the twinning dislocation mediating $\{11\bar{2}1\}$ TB migration should be a two-layer zonal dislocation (see Fig. 1). Obviously, the predicted two-layer zonal twinning dislocation is not observed in our simulation. The TB, when migrating, appears to comprise four or five $\{11\bar{2}1\}$ planes simultaneously (Fig. 5). To better show the structure of the moving TB, a magnified view is displayed in Fig. 9. The color pattern is created by the common neighbor analysis, in which atoms of perfect HCP are colored in red, whereas atoms on the TB are colored in cyan. Note that the cyan atoms are located inside a zone that comprises multiple twinning planes, mostly four layers. Close examination of the TB reveals multiple single-layer steps at the boundary between the red region and the cyan region, as indicated by the blue block arrows. Thus, from this 2D view of the moving TB, it seems that the twin growth is mediated by the motion of single-layered "twinning dislocations".

However, if the single-layered steps are indeed "twinning dislocations", one should be able to identify the dislocation line on the twinning plane. Yet it turns out to be very difficult to capture and visualize the core of individual twinning dislocations that correspond to the single-layered steps by using the analytical tools such as common neighbor analysis, coordination analysis or bond angle analysis. To see if there are twinning dislocation lines on the TB, we first select a thin slice that is parallel to the TB and contains six twinning planes in the parent and CNA is applied to this selected region. Then all the atoms that are on the perfect HCP lattice are deleted. Hence, before twinning, no atoms are left in the pre-selected region and only those atoms on the imperfections such as free surfaces are left, i.e., those atoms on the four sides of the rectangular area (the boundaries of Fig. 10a). Note the viewing direction is along the twinning plane normal. As the twin growth proceeds, the TB is migrating toward the parent and entering the pre-selected region. Atoms on the TB which contains multiple twinning planes start to emerge in the pre-selected region (Fig. 10a). The first $\{11\bar{2}1\}$ twinning plane that emerges in the pre-selected region is denoted as TP_1. Near the top of Fig. 10a, other twinning planes are also emerging, adding on top of TP_1. However, the shape of the boundary of TP_1 that separates TP_1 from the perfect HCP matrix (the blank area) is extremely irregular, and very different from the shape of a typical dislocation line. In dislocation theories, due to the line tension or elastic energy, which scales with Gb^2 (with G being the shear modulus and b the Burgers vector), a dislocation line tends to be an arc or an elliptical loop or tends to straighten out to reduce the line energy. As TP_1 expands, TP_2 that is below TP_1 also grows (Fig. 10b), again with a very irregular boundary shape. Following TP_2, TP_3 and TP_4 also expands and thickens the twinned region (Fig. 10c and d). Note that all these sequentially emerging twinning planes are actually contained in the interface zone and are being transformed into the twin positions. From this analysis, it can be seen that no well-defined dislocation core can be identified during TB migration, although single-layered steps can be seen in the 2D analysis (Fig. 9).

Regarding "twinning dislocations" mediating migration of a $\{11\bar{2}1\}$ TB, Minonishi et al. [6] suggested that the concept of a zonal dislocation was unnecessary to $\{11\bar{2}1\}$ twinning, as the classically defined "zonal dislocation" could not exist on the $\{11\bar{2}1\}$ TB. Instead, a step with a height of one interplanar spacing could exist as a stable fundamental unit. They argued that, along the twinning plane normal direction, there existed two equivalent boundary structures, and these boundary structures on both sides of the unit step were mirrored by the twinning plane. Thus, a single-layered step could be defined as an elementary twinning dislocation.

In explaining the twinning mechanism of $(11\bar{2}1)[11\bar{2}\bar{6}]$ mode in Co, Vaidya and Mahajan [44] proposed the following dislocation reaction for twin nucleation:

$$12\times\frac{1}{12}\left\{\frac{1}{3}\left[\bar{1}\bar{1}26\right]_{(11\bar{2}1)}\right\}\rightarrow 2\left\{\frac{1}{3}\left[\bar{2}113\right]_{(11\bar{2}1)}+\frac{1}{2}\left[1\bar{1}00\right]_{(11\bar{2}1)}\right\} \quad (1)$$

and

$$\left[1\bar{1}00\right]=\frac{1}{3}\left[2\bar{1}\bar{1}0\right]+\frac{1}{3}\left[1\bar{2}10\right] \quad (2)$$

Hence, the total dislocation reaction could be considered a reaction between a $<c+a>=\frac{1}{3}[2\bar{1}\bar{1}3]_{(11\bar{2}1)}$ dislocation and two a dislocations. The elementary twinning dislocation was close to $\frac{1}{36}[\bar{1}\bar{1}26]$. Vaidya and Mahajan suggested that the dislocation reaction in Eq. (2) created a zonal dislocation with its core spreading over twelve consecutive twinning planes, and this zonal dislocation could be a twelve-layer twin embryo. They claimed that this was

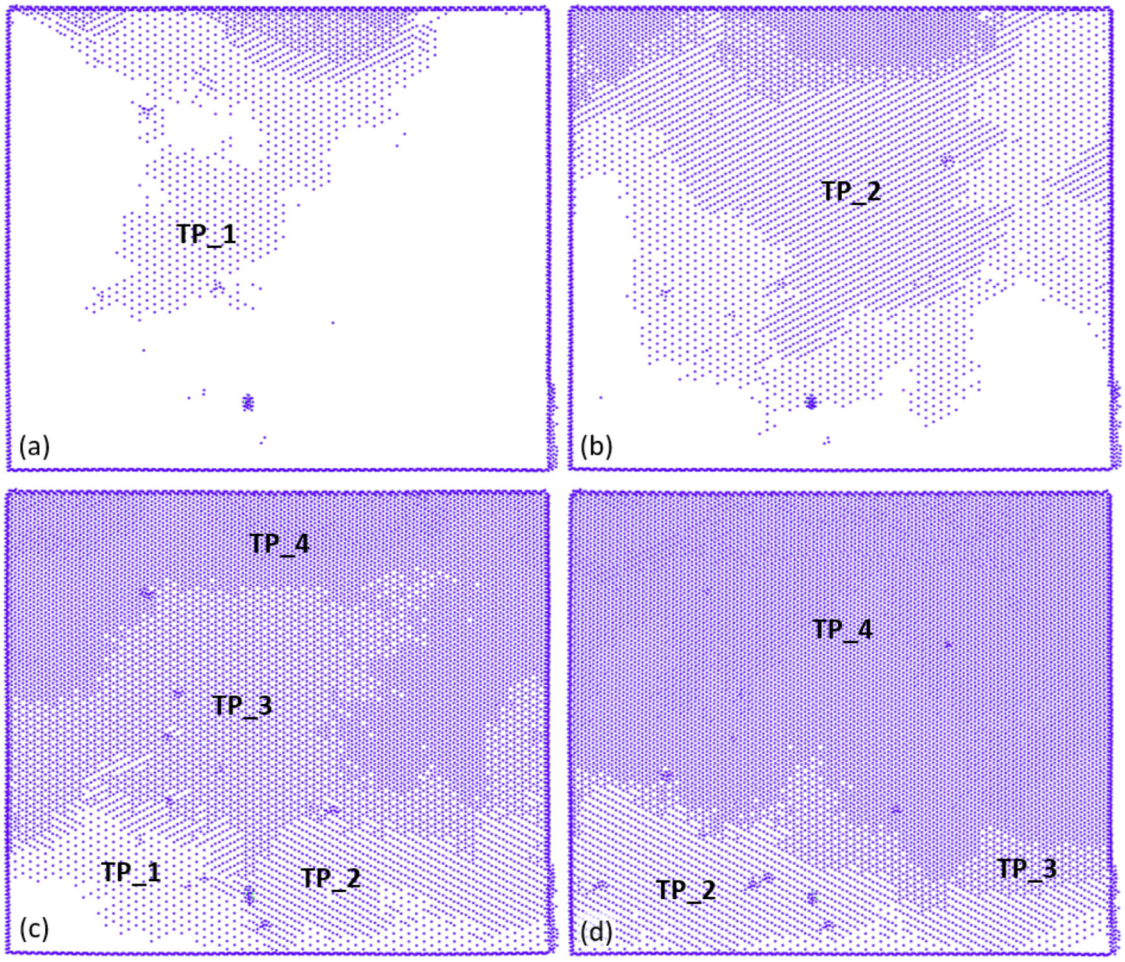

Fig. 10. Progression of twin growth in the simulation. The viewing direction is along the twinning plane normal. These plots are made by first selecting a thin cross section in the parent along the TB normal, then observing how the twin boundary enters the pre-selected region. (a) The first twinning plane TP_1 appears in the region. (b) The second twinning plane TP_2 appears in the region, overlapping with TP_1. (c) and (d) TP_3 and TP_4 are added to the twinned region. Note that the boundary of the twinned area on individual twinning plane is extremely irregular, indicating that no well-defined "twinning dislocation core" can be identified during twin boundary migration.

possible because the interplanar spacing of the twinning plane was rather small ($\frac{1}{2}\gamma \cdot a/\sqrt{4\gamma^2+1} \approx 0.7$ Å). But this mechanism has not been confirmed either by experiments or by atomistic simulations. A zonal dislocation simultaneously containing twelve twinning planes would be very difficult to nucleate, and its subsequent glide for growing a twin embryo would be difficult too.

Despite these models of "twinning dislocations" in the literature, the actual TB migration mechanism is far more complicated due to the complex atomic shuffles that are inevitably involved, especially when large shuffles perpendicular to the direction of twinning shear are needed. In the following, atomic shuffles are analyzed in detail.

4.2. Atomic shuffling during TB migration

Fig. 6-8 show, unambiguously, that complex shuffles must be involved in TB migration. Because the parent prismatic plane should split and reorganize into the prismatic planes of the twin, shuffles in opposite direction but all along the $[1\bar{1}00]$, which is the normal of the plane of shear, should occur. From Fig. 7, when separation and reorganization of parent prismatic planes occur, the shuffling distance along the $[1\bar{1}00]$ should be $\frac{\sqrt{3}a}{12}$, which is about 0.43 Å for atoms on the double layers of individual prismatic planes.

Mininoshi et al. [6] constructed two initial $\{11\bar{2}1\}$ TBs: one configuration in which atoms on both sides of the TB were mirrored; in the other one, the mirror symmetry was disrupted such that an A layer of parent basal extended into a B layer of twin basal. Then these two structures were relaxed. They proposed four possible shuffling mechanisms for migration of an asymmetric $\{11\bar{2}1\}$ TB: (1) shuffling of basal planes by $\frac{1}{2}[1\bar{1}00]$; (2) shuffling of basal planes by $\frac{1}{6}[11\bar{2}0]$; (3) shuffling of basal planes by $\frac{1}{6}1\bar{1}00$; (4) alternate basal planes are displaced in the opposite direction by basal planes by $\frac{1}{12}[1\bar{1}00]$. The first two shuffling mechanisms are unfavorable because the shuffling magnitude is large.

To definitively determine how atoms shuffle during TB migration in our simulation, we examine the evolution of pair distance between two atoms that reside on the same prismatic plane and on two neighboring prismatic planes. In Fig. 11a, a red and a green atom connected by the blue bond are selected, and they reside on two neighboring prismatic planes. The evolution of spacing between these two atoms is computed. Three components along the $[1\bar{1}00]$, $[11\bar{2}6]$, and $(11\bar{2}1)$ normal are plotted. The green curve represents the change in spacing along the $[1\bar{1}00]$, i.e. the zone axis of the twins. Obviously, as the TB migrates and transforms the parent lattice into the twin lattice, a steep drop in the spacing between these two atoms can be seen. Hence, they move towards each other in the opposite direction. In contrast, the component along the $(11\bar{2}1)$ normal (in brown) remains almost constant, indi-

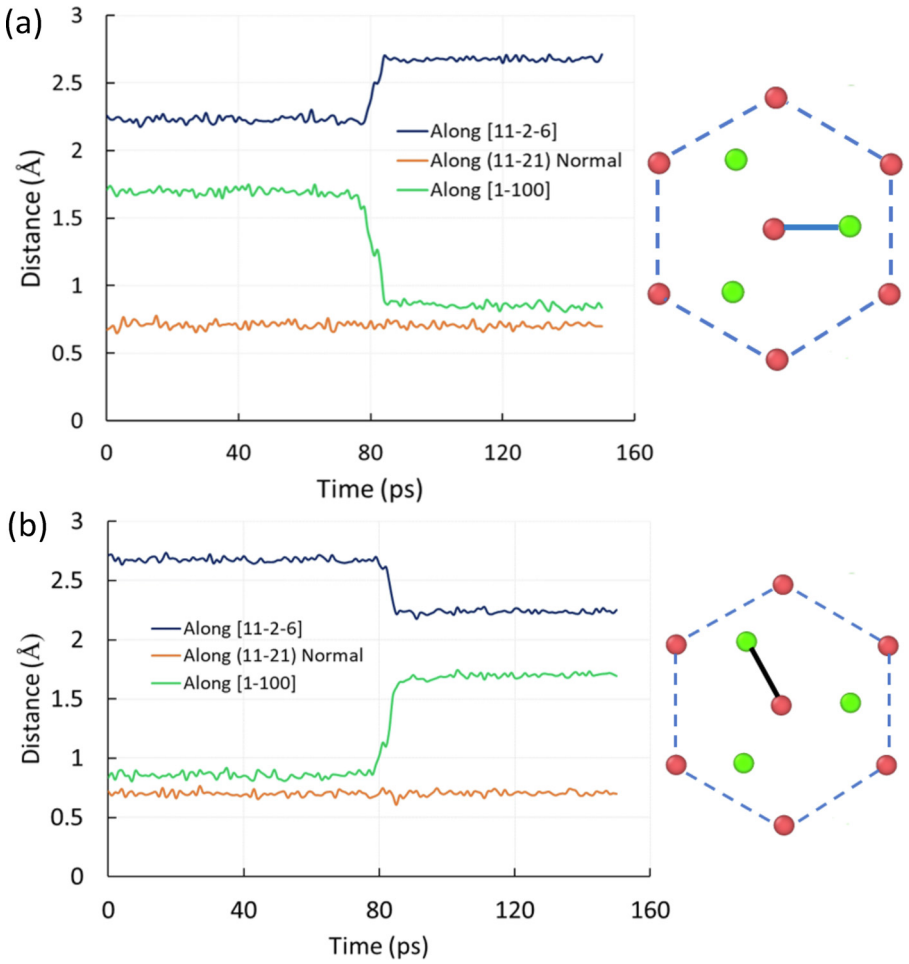

Fig. 11. (a) Evolution of spacing between the red and green atoms (connected by the blue bond) that reside on two neighboring prismatic planes. The spacing along the $[1\bar{1}00]$ decreases after twinning, whereas the spacing along the twinning plane normal remains almost constant. An increase in distance along the $[11\bar{2}\bar{6}]$ can also be seen. (b) Evolution of spacing between the red and green atoms (connected by the black bond) that reside on the double layers of the same prismatic plane. An increase in spacing along the $[1\bar{1}00]$ can be seen, indicating the split of the prismatic plane. A decrease in spacing along the $[11\bar{2}\bar{6}]$ can be seen. (For interpretation of the references to colour in this figure legend, the reader is referred to the web version of this article.)

cating that there is no shuffling along the normal to the twinning plane. However, there is a component along the $[11\bar{2}\bar{6}]$ (in black), i.e. the direction of twinning shear. Along this direction, the spacing increases by ~0.5 Å. In Fig. 11b, a red and a green atom on the same prismatic plane (connected by the black bond) are selected and evolution of their spacing is plotted along the same three directions. The pair spacing increases along the $[1\bar{1}00]$ (the green curve), indicating that these two atoms also move in the opposite direction but away from each other. Again, there is no shuffling along normal direction to the twinning plane (the brown curve). A decrease in spacing along the direction of twinning shear can also be observed. Evolution of position of the two pre-selected atoms in Fig. 11b is shown in Fig. 12. Clearly, they move away from each other, and the displacement of each atom is about ±0.4 Å along the $[1\bar{1}00]$. This distance is close to the theoretical value of $\frac{\sqrt{3}a}{12}$.

4.3. Non-classical behavior of $\{11\bar{2}1\}$ twinning

Fig 7, 8, 11 and 12 in the present work show that the double layers of individual prismatic planes of the parent split and move in the opposite direction towards the neighboring prismatic planes. This process is not energetically favorable, however. From the viewpoint of generalized stacking fault energy, if the red atom in Fig. 11a moves toward the green atom, a very high energy barrier must be overcome, because this direction is opposite to the direction of a Shockley partial dislocation which corresponds to the pathway with the lowest energy barrier [14,16,45,46]. The energy landscape of the basal plane of HCP metals is similar to that of the close-packed {111} planes of FCC metals. The shuffling direction involved in $(11\bar{2}1)[11\bar{2}\bar{6}]$ mode is thus highly unfavorable. However, the actual TB structure circumvents this difficulty.

As shown in Fig. 4, 5 and 7, the actual TB is no longer a crystallographic plane, but a zone that contains multiple $\{11\bar{2}1\}$ planes. To understand this behavior, we show a magnified view of the TB structure during migration in Figure 13. Only two neighboring basal planes are shown, and the viewing direction is now along the [0001] of the parent. Red and green hexagons are drawn to show the stacking sequence in the parent, which has changed after the TB traverses through (Fig. 6). It is clear that, in the interface zone, the hexagonal lattice is distorted. But away from this zone, the distortion in the parent and the twin lattice is minimal. The high energy barrier along the direction against a Shockley partial prevents the parent atoms from shuffling to the twin positions in one step. Instead, to accomplish the shuffles involved in the reorganization of the split columns of atoms of the parent into the twin prismatic planes (Fig. 7), the green and the red atoms gradually move toward the twin positions over multiple twinning planes. Thus, the total shuffling distance along the $[1\bar{1}00]$ is spread over multiple twinning planes in the interface zone. This behavior makes the otherwise difficult shuffling process relatively favor-

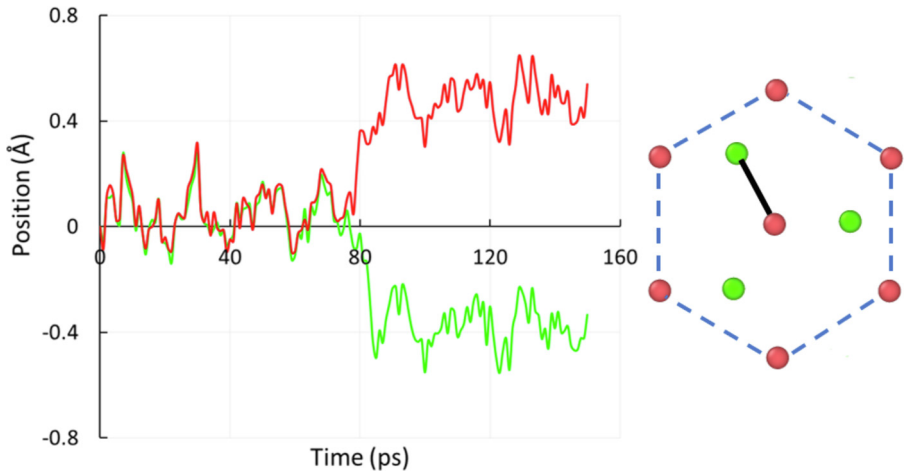

Fig. 12. Evolution of the positions of the red and green atom during twinning. These two atoms move in the opposite direction away from each other along the [1$\bar{1}$00], with displacements about ±0.4 Å. (For interpretation of the references to colour in this figure legend, the reader is referred to the web version of this article.)

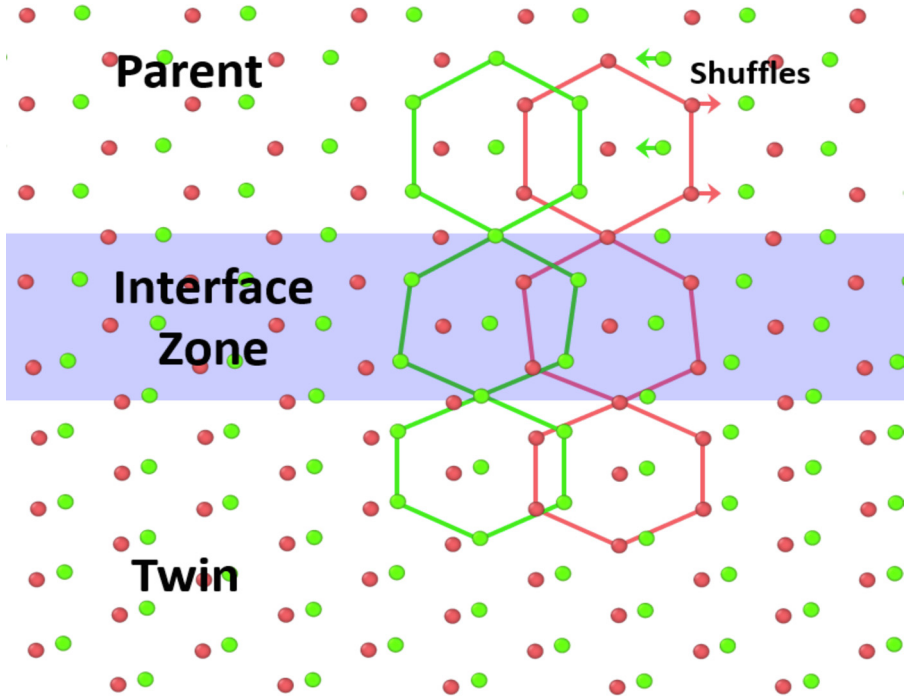

Fig. 13. A magnified view of the interface zone that comprises multiple {11$\bar{2}$1} twinning planes. The viewing direction is along the [0001] of the parent lattice. The red and green arrows indicate the directions of the shuffles that split the prismatic columns of the parent. In the interface zone, the shuffling magnitude gradually increases from the parent to twin until the change in stacking sequence is completed. (For interpretation of the references to colour in this figure legend, the reader is referred to the web version of this article.)

able. Such atomic shuffles must involve all the atoms in the interface zone and require coordinated movements of those atoms. Also, because the direction of shuffling motion is perpendicular to the twinning shear, no well-defined dislocation core on each plane can be identified from the atomistic simulations, although single-layer steps can still be observed on the individual twinning planes in the interface zone, as shown in the 2D view in Fig. 9.

Note that the existence of an interface zone during TB migration is somewhat similar to the concept of "zonal twinning dislocation". A zonal dislocation allows reduction in the magnitude of twinning shear when multiple K_2 planes are involved. Atoms comprised in a zonal dislocation which simultaneously involves multiple twinning planes may move in different directions and displacements [47] in individual planes. Because the displacement of atoms on individual twinning planes in the interface zone is spread over multiple layers, on each of these layers, the atoms do not move to the twin positions and they only arrive at an intermediate position. Thus, the movement of the atoms in the interface zone should be coordinated. In other words, the movement of atoms on a twinning plane must be coupled with the movement of atoms on the other twinning planes in the interface zone. This behavior is reflected in Fig. 14, which plots the evolution of the displacement of a pre-selected atom in the parent lattice. Only the component along the [11$\bar{2}\bar{6}$], i.e. the direction of the external shear, is shown. After twinning, the TB passes through the pre-selected atom, and the displacement remains almost constant. However, before the TB passes through, the displacement presents a characteristic of stick-slip. Note that the overall displacement in each cycle is much larger than the Burgers vector of the theoretical elementary twinning dislocation (0.89 Å), a manifestation of the coordinated movement of the atoms in the interface zone. When all the twinning planes in the interface zone have been transformed to the twin

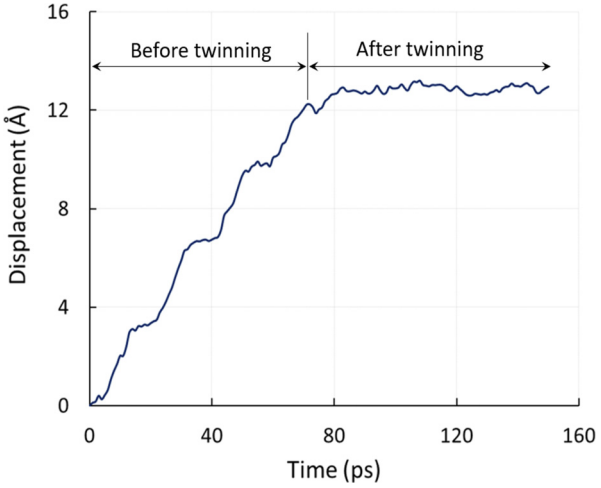

Fig. 14. Evolution of the displacement of a pre-selected atom in the parent along the $[11\bar{2}\bar{6}]$, i.e. the direction of twinning shear. A stick-slip behavior can be seen, indicating that multiple twinning planes are involved in each cycle as the TB migrates.

positions, a relaxation is seen on the displacement curve and this causes the stick-slip type of TB migration.

The simulation results obtained in the present work indicate that, for $\{11\bar{2}1\}$ twinning, when the K_2 plane (0002) is transformed to the K_2' plane by the twinning shear, complex atomic shuffles must be involved. Because of this nature of shuffling, the structure of individual $\{11\bar{2}1\}$ twinning plane cannot be maintained invariant. As seen in Fig. 7, an expansion must be involved along the $[1\bar{1}00]$, i.e. the zone axis of the twins. But in the classical theory, the strain along this direction should be zero, and the twinning plane must be invariant because the parent and the twin lattice are mirrored images of each other about the twinning plane. This feature deviates from the classical twinning behavior in which no structural change should take place to the K_1 and the K_2 plane during TB migration, i.e. the requirement of the invariant plane strain (IPS) condition. However, the deviation is mitigated by the fact that lattice distortion is spread over multiple twinning planes in the interface zone.

Finally, so far there is no experimental observations to verify the asymmetric TB and the twinning behavior in our atomistic simulations. If the electron beam in a TEM experiment is not far away from the direction of twinning shear, the asymmetric TB might be observed by carefully tilting the TEM specimen toward the direction of twinning shear.

5. Conclusions

In the present work, we have performed atomistic simulations to investigate the mechanism for an asymmetric TB migration of $(11\bar{2}1)[11\bar{2}\bar{6}]$ mode. The following conclusions can be reached:

(1) A perfect $\{11\bar{2}1\}$ TB with mirror symmetry cannot exist because of the high repulsive forces between short-bonded atoms on both sides of the TB. As a result, the mirror symmetry breaks down and the stacking sequence in the parent and in the twin differs. This indicates that shuffling must be involved in twin growth, as opposed to the prediction of the classical twinning theory that no shuffles are needed.

(2) During $\{11\bar{2}1\}$ TB migration, the individual $(1\bar{1}00)$ prismatic planes of the parent, which consist of two layers of atoms, split and reorganize into the prismatic planes of the twin. This process is accomplished by shuffles of atoms on the double-layered prismatic planes in the opposite direction along the $[1\bar{1}00]$, i.e. the direction perpendicular to the twinning shear. The energetically unfavorable shuffles are spread over multiple $(11\bar{2}1)$ twinning planes, such that the actual TB is no longer a single atomic plane, but an interface zone. The lattice in the interface zone is distorted.

(3) The TB migration involves multiple twinning planes simultaneously. Single-layer steps can still be seen on individual twinning planes, but no well-defined dislocation core can be identified due to the complex shuffles that are perpendicular to the direction of twinning shear and the resultant lattice distortion in the interface zone.

****

Declaration of Competing Interest

The authors declare that they have no known competing financial interests or personal relationships that could have appeared to influence the work reported in this paper.

Acknowledgement

B.L. gratefully thanks the support from U.S. National Science Foundation (CMMI-2032483, 2016263).

References

[1] B.A. Bilby, A.G. Crocker, The theory of the crystallography of deformation twinning, Proc. R. Soc. Lond. Ser. Math. Phys. Sci. 288 (1965) 240–255, doi:10.1098/rspa.1965.0216.
[2] J.W. Christian, S. Mahajan, Deformation twinning, Prog. Mater. Sci. 39 (1995) 1–157, doi:10.1016/0079-6425(94)00007-7.
[3] E.W. Kelley, W.F. Hosford Jr., Plane-strain compression of magnesium and magnesium alloy crystals, Trans. Metallurg. Soc. AIME 242 (1968) 5–13.
[4] M.L. Kronberg, A structural mechanism for the twinning process on {101²} in hexagonal close packed metals, Acta Metall. 16 (1968) 29–34, doi:10.1016/0001-6160(68)90068-0.
[5] B. Li, H. El Kadiri, M.F. Horstemeyer, Extended zonal dislocations mediating twinning in titanium, Philos. Mag. 92 (2012) 1006–1022, doi:10.1080/14786435.2011.637985.
[6] Y. Minonishi, S. Ishioka, M. Koiwa, S. Mobozumi, The structure of {1121} twin boundaries in H.C.P. crystals, Phys. Status Solidi A 71 (1982) 253–258, doi:10.1002/pssa.2210710130.
[7] X.Y. Zhang, B. Li, J. Tu, Q. Sun, Q. Liu, Non-classical twinning behavior in dynamically deformed cobalt, Mater. Res. Lett. (2015) In press.
[8] B. Li, E. Ma, Zonal dislocations mediating {10-11}<10-1-2>twinning in magnesium, Acta Mater. 57 (2009) 1734–1743, doi:10.1016/j.actamat.2008.12.016.
[9] J. Wang, J.P. Hirth, C.N. Tomé, {-1012} Twinning nucleation mechanisms in hexagonal-close-packed crystals, Acta Mater. 57 (2009) 5521–5530, doi:10.1016/j.actamat.2009.07.047.
[10] A. Serra, D.J. Bacon, Computer simulation of twin boundaries in the H.C.P. metals, Philos. Mag. A 54 (1986) 793–804, doi:10.1080/01418618608244438.
[11] D.G. Westlake, Twinning in zirconium, Acta Metall. 9 (1961) 327–331, doi:10.1016/0001-6160(61)90226-7.
[12] X.Y. Zhang, B. Li, X.L. Wu, Y.T. Zhu, Q. Ma, Q. Liu, P.T. Wang, M.F. Horstemeyer, Twin boundaries showing very large deviations from the twinning plane, Scr. Mater. 67 (2012) 862–865, doi:10.1016/j.scriptamat.2012.08.012.
[13] X. Zhang, B. Li, Q. Liu, Non-equilibrium basal stacking faults in hexagonal close-packed metals, Acta Materialia. 90 (2015) 140–150.
[14] B. Li, B.Y. Cao, K.T. Ramesh, E. Ma, A nucleation mechanism of deformation twins in pure aluminum, Acta Mater. 57 (2009) 4500–4507, doi:10.1016/j.actamat.2009.06.014.
[15] S. Mahajan, G.Y. Chin, Formation of deformation twins in F.C.C. crystals, Acta Metall. 21 (1973) 1353–1363, doi:10.1016/0001-6160(73)90085-0.
[16] S. Kibey, J.B. Liu, D.D. Johnson, H. Sehitoglu, Predicting twinning stress in FCC metals: linking twin-energy pathways to twin nucleation, Acta Mater. 55 (2007) 6843–6851, doi:10.1016/j.actamat.2007.08.042.
[17] S. Mendelson, Zonal dislocations and twin lamellae in H.C.P. metals, Mater. Sci. Eng. 4 (1969) 231–242, doi:10.1016/0025-5416(69)90067-6.
[18] S. Mendelson, Dissociations in HCP metals, J. Appl. Phys. 41 (1970) 1893–1910, doi:10.1063/1.1659139.
[19] N. Thompson, D.J. Millard XXXVIII, Twin formation, in cadmium, Philos. Mag. Ser. 43 (1952) 422–440, doi:10.1080/14786440408520175.
[20] B.-Y. Liu, J. Wang, B. Li, L. Lu, X.-Y. Zhang, Z.-W. Shan, J. Li, C.-L. Jia, J. Sun, E. Ma, Twinning-like lattice reorientation without a crystallographic twinning plane, Nat. Commun. 5 (2014), doi:10.1038/ncomms4297.
[21] B. Li, E. Ma, Atomic shuffling dominated mechanism for deformation twinning in magnesium, Phys. Rev. Lett. 103 (2009) 035503, doi:10.1103/PhysRevLett.103.035503.

[22] J. Li, M. Sui, B. Li, A half-shear-half-shuffle mechanism and the single-layer twinning dislocation for {11-22}⟨11-2-3⟩ mode in hexagonal close-packed titanium, Acta Mater 216 (2021) 117150, doi:10.1016/j.actamat.2021.117150.
[23] A. Serra, D.J. Bacon, Modelling the motion of {1122} twinning dislocations in the HCP metals, Mater. Sci. Eng. A 400–401 (2005) 496–498, doi:10.1016/j.msea.2005.01.067.
[24] B. Li, X. Zhang, Twinning with zero twinning shear, Scripta Materialia. (2016) in press.
[25] J. Kacher, A.M. Minor, Twin boundary interactions with grain boundaries investigated in pure rhenium, Acta Mater. 81 (2014) 1–8, doi:10.1016/j.actamat.2014.08.013.
[26] G.C. Kaschner, C.N. Tomé, I.J. Beyerlein, S.C. Vogel, D.W. Brown, R.J. McCabe, Role of twinning in the hardening response of zirconium during temperature reloads, Acta Mater. 54 (2006) 2887–2896, doi:10.1016/j.actamat.2006.02.036.
[27] G.C. Kaschner, C.N. Tomé, R.J. McCabe, A. Misra, S.C. Vogel, D.W. Brown, Exploring the dislocation/twin interactions in zirconium, Mater. Sci. Eng. A 463 (2007) 122–127, doi:10.1016/j.msea.2006.09.115.
[28] F. Xu, X. Zhang, H. Ni, Q. Liu, Deformation twinning in pure Ti during dynamic plastic deformation, Mater. Sci. Eng. A 541 (2012) 190–195, doi:10.1016/j.msea.2012.02.021.
[29] N. Stanford, Observation of 1121 twinning in a Mg-based alloy, Philos. Mag. Lett. 88 (2008) 379–386, doi:10.1080/09500830802070793.
[30] A. Serra, R.C. Pond, D.J. Bacon, Computer simulation of the structure and mobility of twinning disclocations in H.C.P. Metals, Acta Metall. Mater. 39 (1991) 1469–1480, doi:10.1016/0956-7151(91)90232-P.
[31] H.A. Khater, A. Serra, R.C. Pond, Atomic shearing and shuffling accompanying the motion of twinning disconnections in zirconium, Philos. Mag. 93 (2013) 1279–1298, doi:10.1080/14786435.2013.769071.
[32] R.R. Zope, Y. Mishin, Interatomic potentials for atomistic simulations of the Ti-Al system, Phys. Rev. B 68 (2003) 024102, doi:10.1103/PhysRevB.68.024102.
[33] M.S. Daw, M.I. Baskes, Semiempirical, quantum mechanical calculation of hydrogen embrittlement in metals, Phys. Rev. Lett. 50 (1983) 1285–1288, doi:10.1103/PhysRevLett.50.1285.
[34] M.S. Daw, M.I. Baskes, Embedded-atom method: Derivation and application to impurities, surfaces, and other defects in metals, Phys. Rev. B 29 (1984) 6443–6453, doi:10.1103/PhysRevB.29.6443.
[35] B. Li, Reply to the two comments, by A. Serra, D. J. Bacon and R. C. Pond, and by H. El Kadiri and C. Barrett on B. Li, H. El Kadiri and M.F. Horstemeyer "extended zonal dislocations mediating twinning in titanium,", Philos. Mag. 93 (2013) 3504–3510, doi:10.1080/14786435.2013.815818.
[36] S. Plimpton, Fast parallel algorithms for short-range molecular dynamics, J. Comput. Phys. 117 (1995) 1–19, doi:10.1006/jcph.1995.1039.
[37] A. Stukowski, Visualization and analysis of atomistic simulation data with OVITO–the open visualization tool, Model. Simul. Mater. Sci. Eng. 18 (2010) 015012, doi:10.1088/0965-0393/18/1/015012.
[38] S. Nosé, A unified formulation of the constant temperature molecular dynamics methods, J. Chem. Phys. 81 (1984) 511–519, doi:10.1063/1.447334.
[39] W.G. Hoover, Canonical dynamics: equilibrium phase-space distributions, Phys. Rev. A 31 (1985) 1695–1697, doi:10.1103/PhysRevA.31.1695.
[40] J.Dana. Honeycutt, H.C. Andersen, Molecular dynamics study of melting and freezing of small Lennard-Jones clusters, J. Phys. Chem. 91 (1987) 4950–4963, doi:10.1021/j100303a014.
[41] P.G. Partridge, E. Roberts, The formation and behaviour of incoherent twin boundaries in hexagonal metals, Acta Metall 12 (1964) 1205–1210, doi:10.1016/0001-6160(64)90103-8.
[42] M.A. Gharghouri, G.C. Weatherly, J.D. Embury, The interaction of twins and precipitates in a Mg-7.7 at.% Al alloy, Philos. Mag. A 78 (1998) 1137–1149, doi:10.1080/01418619808239980.
[43] X.Y. Zhang, B. Li, J. Tu, Q. Sun, Q. Liu, Non-classical twinning behavior in dynamically deformed cobalt, Mater. Res. Lett. 3 (2015) 142–148, doi:10.1080/21663831.2015.1034297.
[44] S. Vaidya, S. Mahajan, Accommodation and formation of {11-21} twins in Co single crystals, Acta Metall. 28 (1980) 1123–1131, doi:10.1016/0001-6160(80)90095-4.
[45] V. Vítek, Intrinsic stacking faults in body-centred cubic crystals, Philos. Mag. 18 (1968) 773–786, doi:10.1080/14786436808227500.
[46] E.B. Tadmor, N. Bernstein, A first-principles measure for the twinnability of FCC metals, J. Mech. Phys. Solids. 52 (2004) 2507–2519, doi:10.1016/j.jmps.2004.05.002.
[47] J.P. Hirth, J. Lothe, Theory of Dislocations: 2nd (second) Edition, Krieger Publishing Company, 1983.